Journal of Materials Chemistry B

Accepted Manuscript

This article can be cited before page numbers have been issued, to do this please use: Y. Wang, C. Hou, Y. Zhang, F. He, M. Liu and X. Li, *J. Mater. Chem. B*, 2016, DOI: 10.1039/C6TB00276E.

ROYAL SOCIETY OF CHEMISTRY

www.rsc.org/materialsB

View Article Online
DOI: 10.1039/C6TB00276E

Preparation of graphene nano-sheets bonded PDA/MOFs microcapsules immobilized glucose oxidase as mimetic multi-enzyme system for electrochemical sensing of glucose

Yang Wang, Chen Hou, Yun Zhang *, Fu He, Mingzhu Liu*, Xiaoli Li

State Key Laboratory of Applied Organic Chemistry, Key Laboratory of Nonferrous Metal Chemistry and Resources Utilization of Gansu Province, College of Chemistry and Chemical Engineering, College of Resources and Environment, Institute of Biochemical Engineering &Environmental Technology, Gansu Key Laboratory for Environmental Pollution Prediction and Control, College of Earth and Environmental Sciences, Lanzhou University, Lanzhou 730000, China

Abstract

A novel amperometric biosensor for glucose detection was fabricated based on the mimetic multi-enzyme system by combing the mimetic enzyme (metal-organic frameworks, MOFs) and glucose oxidase (GOx). The microcapsule constructed with polydopamine (PDA) and ZIF-8 using $CaCO_3$ templates could be utilized not only to provide the biocompatible and non-toxic microenvironment to immobilized GOx, but also as the efficient mimetic enzyme because of the peroxidase-like property of ZIF-8. The graphene nano-sheets (rGO) were bonded to PDA/ZIF-8 microcapsules to accelerate the electron transfer between microcapsule and electrode, and the resulted PDA/ZIF-8@rGO showed excellent electro-catalytic activity towards H_2O_2. The mimetic multi-enzyme system was fabricated when GOx was immobilized in the

*Corresponding author. Fax: 86-931-8912113; *E-mail address*: zhangyun@lzu.edu.cn (Y. Zhang)
*Corresponding author. Fax: 86-931-8912582; *E-mail address*: mzliu@lzu.edu.cn (M.Z. Liu)

View Article Online
DOI: 10.1039/C6TB00276E

as-prepared microcapsule, and the developed GOx/PDA/ZIF-8@rGO/GCE biosensor exhibited extraordinary electro-detection performance for glucose with two wide linear ranged from 1μM to 1.2 mM and 1.2 mM to 3.6 mM, and the limit of detection was 0.333 μM (S/N=3). Moreover, the good selectivity for glucose and satisfactory results in real samples detection by the prepared biosensor were also demonstrated.

1.Introduction

The rapid, sensitive and accurate measurement to detect the trace amount of glucose is of extreme importance in clinical diagnose, food industry and particularly in diabetes mellitus, thus many methods have been applied in glucose detection like HPLC, fluorimetry and electrochemistry analysis.[1] Electrochemical methods for glucose detection using both enzymatic and nonenzymatic sensing techniques have garnered significant interest due to their capacity to achieve continuous glucose monitoring.[2] Combining both the advantages of electrochemical techniques and the specificity of enzymes, the electrochemical detection based on enzymatic sensors show great potential applications among these methods in diabetes blood glucose test due to their high sensitivity, selectivity, portability, linearity, rapidness and low cost.[3,4] The major challenge in constructing a glucose biosensor is suitable immobilization of glucose oxidase (GOx) on electrode through effective electrical communication between immobilized enzymes and electrodes.[5] Therefore, searching for some new materials and methods which are used for surface modification of electrodes to improve the sensitivity, selectivity and stability of the biosensors is still an urgent task.

View Article Online
DOI: 10.1039/C6TB00276E

Protein capsules with tailored structures and properties have been intrigued increasing interests from scientific researches to technological applications, especially in enzyme immobilization.[6,7] Fabrication of protein microcapsules based on layer-by-layer (LBL) method by $CaCO_3$ templates have shown high efficient for enzyme immobilization with well biocompatible and non-toxic microenvironment as reported. PDA as a wall component provides a simple, green and efficient approach to form a biocompatible micro-bioreactor with a thick-controllable, uniform and interconnectivity outer shell.[8,9] Thus, the PDA could be the ideal candidate to prepare microcapsules used in immobilization of enzyme.[10] However, no works used PDA-based microcapsules immobilized enzyme to construct electrochemical enzyme sensor so far as we know.

Multi-enzyme systems involving consecutive series of enzymatic reactions proceeding have caused great interests in latest years.[11] Metal-organic frameworks (MOFs) with fascinating structures and intriguing properties always are considered as extraordinary drug delivery, gas storage and separation, and preconcentration materials. MOFs have also been tryed to apply as electrode materials for efficiently detecting biologically related compounds.[12] Recently it has captured interest as mimetic enzyme due to its outstanding peroxidase-like catalytic activity.[13] Co-operation of MOFs as mimetic enzyme and natural enzyme, the new kind of biomimetic multi-enzyme systems could be established.[14] Hou and co-workers reported the construction of the mimetic multi-enzyme systems by embedding GOx in a mimetic peroxidase zeolitic imidazolate framework 8 (ZIF-8) and used as

View Article Online
DOI: 10.1039/C6TB00276E

biosensors for glucose detection.[15] Although MOFs have shown great potential in electrochemical biosensor field benefited from its electrochemical activity and large surface area, the glucose electrochemical sensor fabricated by MOFs-enzyme multi-enzyme systems is rarely reported.

Herein, the novel electrochemical enzyme sensor was fabricated by introducing the mimetic multi-enzyme system based on MOFs and GOx into glucose electro-detection. In typical, the GOx was captured by $CaCO_3$ templates in the co-precipitation process and released in the PDA/ZIF-8 microcapsule after removing templates. To obtain better electrochemical activity and higher accessible surface area and conductivity, graphene nano-sheets were binded to PDA/ZIF-8 microcapsule by cooperative interaction via π-π stacking and hydrogen bonding with ZIF-8.[16.17] Finally, the resulted PDA/ZIF-8@graphene microcapsule was immobilized on a glassy carbon electrode (GCE) to form a sensing platform for the detection of glucose with multi-enzyme system which co-operated the GOx and mimetic enzyme (ZIF-8). The results demonstrated the promising applications of enzyme microcapsule in electrochemical field, and opened a new avenue for extending the electrochemical enzyme biosensor of the mimetic multi-enzyme system.

2. Experiment

2.1. Materials and Reagents

$Zn(NO_3)_2 \cdot 6H_2O$ and 2-methylimidazole, were purchased from Aihua Fine Chemicals Co., Ltd. (China); Glucose oxidase (GOx, Type VII, 50 KU) was purchased from Sigma Chemical Co.; Dopamine hydrochloride, Tris(hydroxymethyl)-amiomethane

View Article Online
DOI: 10.1039/C6TB00276E

(Tris), ethylenediamine tetraacetic acid disodium (EDTA), hydrochloric acid (HCl), and other chemicals and reagents were analytical grade, obtained from Tianjing Chemical Reagent Company (China).

2.2. Apparatus

The FT-IR was recorded with a Nicolet Magna-IR spectrophotometer between 4000 and 450 cm^{-1} using the KBr pellet technique. Transmission electron microscopy (TEM, FEI Tecnai G20) was obtained to elucidate the dimensions of the nanoparticle. The crystalline structures of samples were characterized by X-ray diffraction (XRD) (RigakuD/max-2400). Amperometric measurements were performed on a CHI 660E electrochemical workstation.

2.3 Preparation of $CaCO_3$ microparticles

$CaCO_3$ microparticles were prepared according to the previous report.[10] Typically, 0.33 M Na_2CO_3 solution was poured into an equal volume of 0.33 M $CaCl_2$ solution rapidly, and stirred with intense agitation on a magnetic stirrer for 30 seconds at room temperature. After settling without stirring for another 10 minutes, the white precipitate was filtered off, washed with deionized water and ethanol throughly, then dried in air for 24 h.

2.4 Preparation of magnetic $CaCO_3$@PDA/ZIF-8 microparticles

To prepare the $CaCO_3$@PDA microparticles, 100 mg of $CaCO_3$ microparticles were suspended in Tris-HCl buffer (40 ml, 50 mM, pH 8.5) containing a concentration of 2 mg ml^{-1} of dopamine hydrochloride with constant stirring. After polymerization for 8 h, the $CaCO_3$@PDA microparticles were obtained.

View Article Online
DOI: 10.1039/C6TB00276E

To prepare $CaCO_3$@PDA/ZIF-8 microparticles, a certain amount of obtained $CaCO_3$@PDA microparticles were suspended in 6.5 ml of 50% ethanol solution containing 2.9 mmol $Zn(NO_3)_2$ and stirred for 30 min. Then 8.5 ml of 50% ethanol solution containing 12 mmol 2-methylimidazole was added to the above suspension. The $CaCO_3$@PDA/ZIF-8 microparticles were obtained after reactioin for 30 min, and the products were centrifuged, followed by washing with deionized water and ethanol three times, and drying at 40 °C in an oven under vacuum for 24 h.[18,19]

2.5 Preparation of PDA/ZIF-8@rGO microcapsules

Reduced graphite oxides nano-sheets (rGO) suspension was prepared according to the modified Hummers method.[20] 0.15 g of $CaCO_3$@PDA/ZIF-8 microparticles were added to graphene suspension with stirring for 3 h and $CaCO_3$@PDA/ZIF-8@rGO microparticles were collected by centrifugation. To remove the template, the resulted microparticles were stirred in 0.1 M EDTA solution at room tempreture for 30 min. After $CaCO_3$ microparticles were removed, the final products, PDA/ZIF-8@rGO microcapsules, were washed thoroughly with deionized water and ethanol and dried at 60 ^{o}C for 24 h under vacuum.

The PDA/ZIF-8 microcapsules were obtained after the $CaCO_3$ microparticles were removed with 0.1 M EDTA solution at room tempreture.

The GOx immobilzed PDA/ZIF-8@rGO microcapsules were prepared in processes. GOx (fianl concentration is 1.5 mg ml^{-1}) was dissolved in 1 ml of Tris-HCl buffer solution (50 mM, pH 7.0), and added into 4 ml of 0.33 M $CaCl_2$ solution. The following procedures were the same as the preparation of PDA/ZIF-8@rGO

View Article Online
DOI: 10.1039/C6TB00276E

microcapsules, the final obtained products were abbreviated to GOx/PDA/ZIF-8@rGO. The procedure of preparation of GOx/PDA/ZIF-8 microcapsule was shown in Fig. 1.

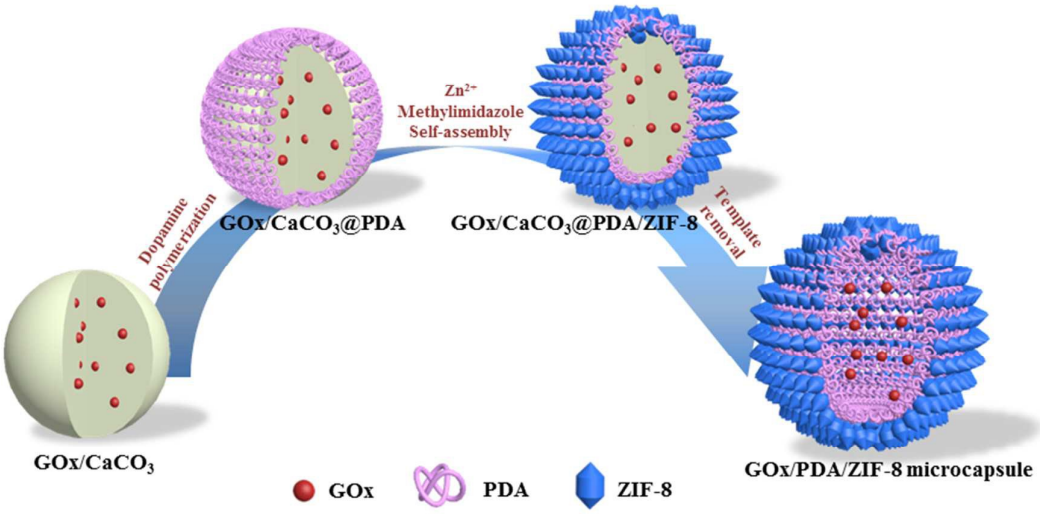

Fig. 1. Scheme for the preparation of GOx/PDA/ZIF-8 microcapsules.

2.6 Fabrication of glucose biosensor

1 mg/mL of GOx/PDA/ZIF-8@rGO suspension was prepared by dispersing GOx/PDA/ZIF-8@rGO into double distilled water. Then 5 μL of above suspension was coated onto the GCE (polished to a mirror finish sequentially with 1.0, 0.3 mm and 0.05 μm of alumina powder), and dried at 4 ^{o}C for 8 h. Finally, the obtained electrode was washed with double distilled water, and 5 μL Nafion solution was coated on the surface. The resulted GOx/PDA/ZIF-8@rGO/GCE was stored in phosphate buffer solution (PBS, 0.1 M, pH=7.0) at 4 ^{o}C when not in use. For comparison, PDA/ZIF-8@rGO/GCE and PDA/ZIF-8/GCE were also prepared by dropping 5 μL of PDA/ZIF-8@rGO and PDA/ZIF-8 solutions on the surface of GCE, respectively.

View Article Online
DOI: 10.1039/C6TB00276E

3. Results and discussion

3.1. Characterization of PDA/ZIF-8@rGO microcapsules

The as-prepared $CaCO_3$ microparticle presented an average size of 4 μm, and PDA polymerization lead to a uniform coating layer of 12 nm after reacting with $CaCO_3$ microparticle, as observed in Fig. 2a and b. Then we examined the growth of ZIF-8 on $CaCO_3$@PDA microparticle. As can be seen from Fig. 2c and d, ZIF-8 nucleated on the surface of PDA coating and subsequently grew into large nanocrystals. The as-prepared $CaCO_3$@PDA/ZIF-8 presents a robust shell (about 200 nm) on top of the $CaCO_3$ microparticle (Fig. 2d). The strong chelating interaction of catechol groups in PDA with Zn ions and the hydrophobic interaction between aromatic groups of PDA and the organic ligands facilitated rapid nucleation of metal-organic frameworks, leading to high yield of the well-coated hybrid shell. After template removal, the transparent PDA/ZIF-8 microcapsule formed with the rough organic-inorganic hybrid shell (Fig. 2e). Due to the outer coating of metal-organic frameworks, the as-prepared PDA/ZIF-8 microcapsule held the plump, spherical structure and prevented collapse and fold upon a large cavity. As can be seen from Fig. 2f, it is obviously the folded graphene nano-sheets combined with PDA/ZIF-8 microcapsule after graphene nano-sheets were bound to microcapsule, demonstrated the PDA/ZIF-8@rGO has been successfully prepared. The presented elements in $CaCO_3$@PDA/ZIF-8 microparticle and PDA/ZIF-8 microcapsule were confirmed by energy-dispersive x-ray spectroscopy (EDS) (Fig. 2g, h). Characteristic peaks of Zn confirmed the existence of ZIF-8, and peaks of C and O can be assigned to PDA and ZIF-8.

View Article Online
DOI: 10.1039/C6TB00276E

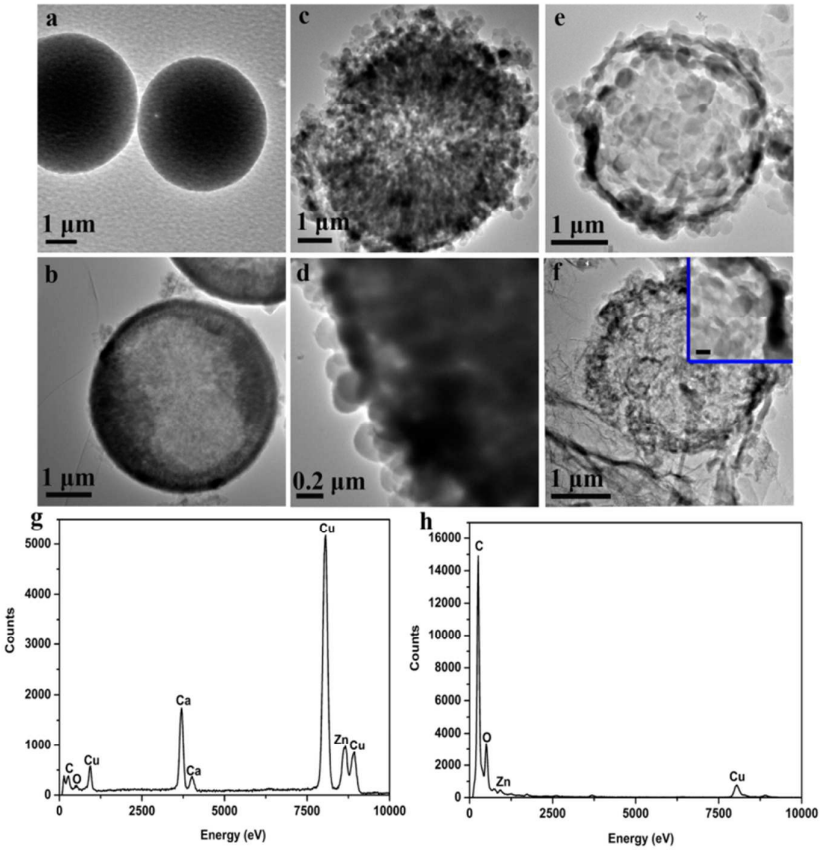

Fig. 2. TEM images of $CaCO_3$ microparticle (a), $CaCO_3$@PDA microparticle (b), $CaCO_3$@PDA/ZIF-8 microparticle (c and d), PDA/ZIF-8 microcapsule (e) and PDA/ZIF-8@rGO composite (f). The scale bar of the insert of f is 0.2 μm; EDS analysis of $CaCO_3$@PDA/ZIF-8 microparticle (g) and PDA/ZIF-8 microcapsule (h) (The signals of Cu and part of C/O are from the formvar-carbon coated copper grid.).

The FT-IR spectrum of $CaCO_3$@PDA, $CaCO_3$@PDA/ZIF-8 microparticle and PDA/ZIF-8 microcapsule is presented in Fig. 3. A typical peak of 870 cm^{-1} was shown in the spectrum of $CaCO_3$@PDA and $CaCO_3$@PDA@ZIF-8, which was attributed to vaterite polymorphs of pure-$CaCO_3$.[10] After template removal, the quondam suppressed peaks originated from PDA and ZIF-8 appeared. New peak at 1600 cm^{-1} can be attributed to the benzene ring C-C vibration of PDA. Adsorption

View Article Online
DOI: 10.1039/C6TB00276E

peaks at 1477 and 998 cm^{-1} are associated to the stretching and plane bending of imidazole ring, respectively. The bands at 1200 and 1124 cm^{-1} are due to the C-O asymmetric vibration and C-N stretching vibration of phenol compounds. The band at 450 cm^{-1} is assigned to Zn-N stretch. In addition, the broad adsorption peak at 3400 cm^{-1} can be resulted from the overlapping of hydroxyls, adsorbed water and amines of PDA@ZIF-8.[21,22]

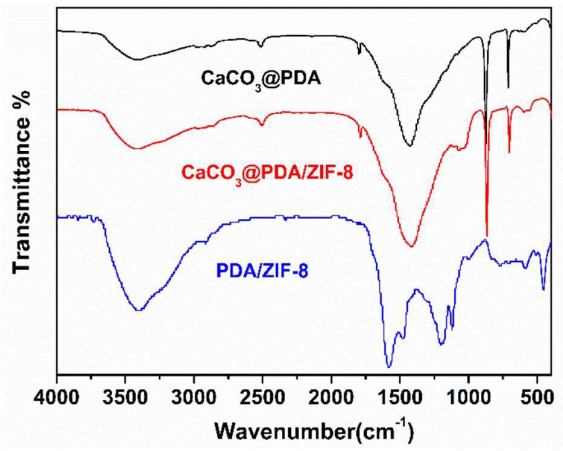

Fig. 3. FT-IR spectrum of $CaCO_3$@PDA, $CaCO_3$@PDA/ZIF-8 microparticle and PDA/ZIF-8 microcapsule.

The XRD patterns of $CaCO_3$@PDA, $CaCO_3$@PDA/ZIF-8 microparticle and PDA/ZIF-8 microcapsule are displayed by Fig. 4. As can be seen from Fig. 4, XRD patterns of $CaCO_3$@PDA and $CaCO_3$@PDA/ZIF-8 microparticle presented the same characteristic peaks with $CaCO_3$ microparticle,[23] the peaks of ZIF-8 didn't observed due to relative high amount of $CaCO_3$ component in $CaCO_3$@PDA/ZIF-8 microparticle. After template removal, peaks of PDA/ZIF-8 microcapsule appeared and exhibited no significant difference with regard to the crystal structure and crystallinity with ZIF-8,[24] the broad peak centered at 25° can be assigned to pure PDA,

View Article Online
DOI: 10.1039/C6TB00276E

which is a typical characteristic peak of the polymer.[25] The XRD pattern of PDA@ZIF-8 indicated the successful crystallization of ZIF-8 on PDA polymer.

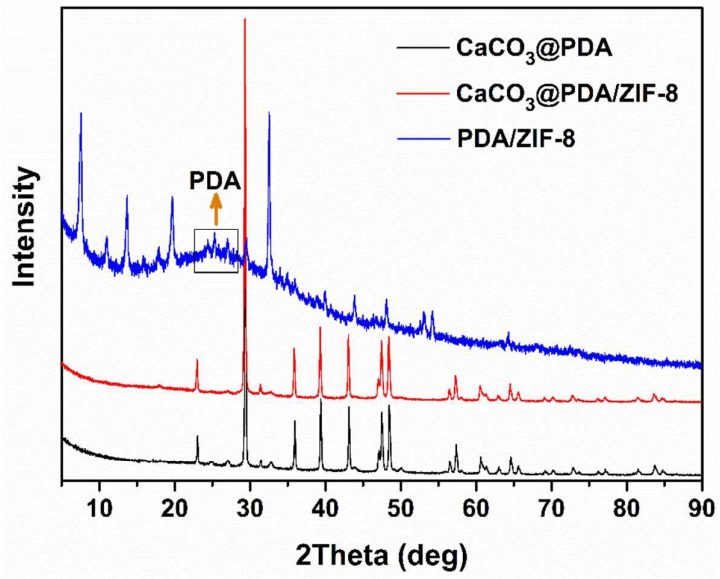

Fig. 4. XRD spectrum of $CaCO_3$@PDA, $CaCO_3$@PDA/ZIF-8 and PDA/ZIF-8 microcapsule.

3.2. Electrochemical detection mechanism of glucose on PDA/ZIF-8@rGO/GCE

In preliminary experiment, we anticipated to fabricate the mimetic multi-enzyme system with consecutive series of enzymatic reactions. In the microcapsule constructed micro-reactor, glucose was oxidized by GOx to produce H_2O_2, and then H_2O_2 was reduced by ZIF-8 due to the mimetic horseradish peroxidase property.[26] The mechanism was shown in Fig. 5. Firstly, glucose was infiltrated into PDA microcapsule, and catalyzed by the inside GOx to produce glucose acid and H_2O_2. After H_2O_2 was flowed out, the outside peroxidase-like ZIF-8 catalyzed H_2O_2 to H_2O immediately, the catalysis also caused receiving and losing electrons between ZIF-8 and electrode at the same time. In this process, the graphene nano-sheets could enhance the electron exchange from ZIF-8 to electrode and accelerate the electron

View Article Online
DOI: 10.1039/C6TB00276E

transport.

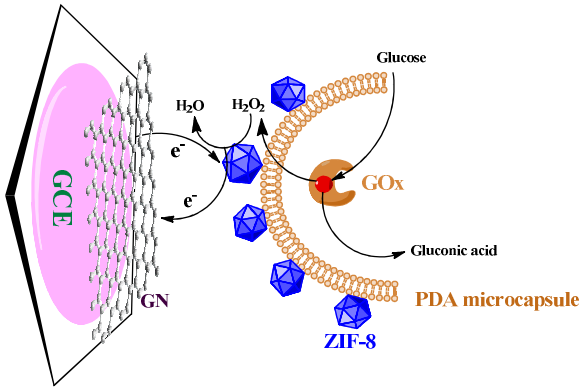

Fig. 5. The mechanism of GOx/PDA/ZIF-8@rGO/GCE for glucose detection.

3.3. Electrochemical detection of H_2O_2 on PDA/ZIF-8@rGO/GCE

In order to verify the mimetic peroxidase property of the PDA/ZIF-8@rGO, the electrochemical behaviors of H_2O_2 were carried out on the PDA/ZIF-8@rGO/GCE. Cyclic voltammograms of bare GCE, the PDA/ZIF-8/GCE, and the PDA/ZIF-8@rGO/GCE in phosphate buffer solution (0.1 M, pH 7.0) containing 1 mM H_2O_2 were studied, and the results were shown in Fig. 6. On the bare GCE, the small anodic peak current of H_2O_2 oxidation indicates it is inefficient to detect of H_2O_2. Because of the peroxidase-like catalytic activity of MOFs, the anodic peak current of H_2O_2 oxidation enhanced notable at PDA/ZIF-8/GCE. Nevertheless, the oxidation current by the PDA/ZIF-8/rGO/GCE was obviously higher than those of the bare GCE and PDA/ZIF-8/GCE, which indicated the combination of graphene nano-sheets and ZIF-8 improved the sensitivity of H_2O_2. Took the advantages of the excellent electrical conductivity of graphene nano-sheets, and the unique properties of MOFs like large surface area, the relative surface area of electrode can be increased significantly, thus improved the electro-catalytic ability for H_2O_2 of the as-prepared

View Article Online
DOI: 10.1039/C6TB00276E

composite. Therefore, the PDA/ZIF-8@rGO/GCE exhibited the extraordinary electro-catalysis for H_2O_2.

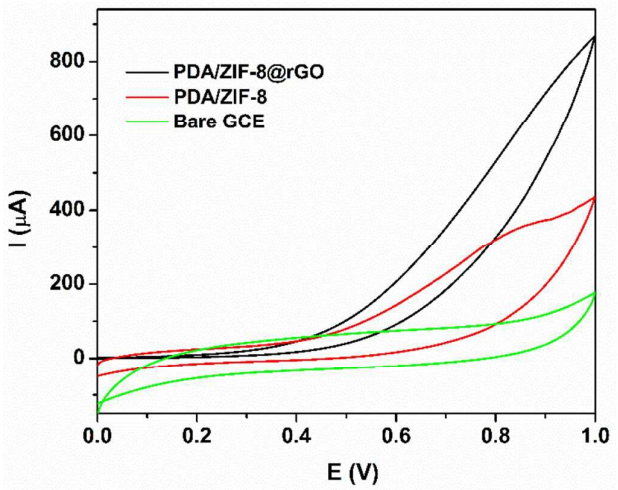

Fig. 6. Cyclic voltammograms at the bare GCE, the PDA/ZIF-8/GCE, and the PDA/ZIF-8@rGO/GCE in the presence of H_2O_2 in PBS (0.1M, pH 7.0). H_2O_2 concentration: 1 mM, and scan rate: 50 mV s^{-1}

The PDA/ZIF-8@rGO/GCE for the electrochemical detection of H_2O_2 was measured by recording the amperometric response of prepared sensor with successive addition of H_2O_2 to the stirring PBS (0.1 M, pH 7.0). As shown in Fig. 7, the oxidation current increased with the increase of H_2O_2 concentration, and the as-prepared biosensor exhibited fast and well defined response towards H_2O_2 additions, the proposed current reached a maximum steady state value and achieved 95% of steady-state current within 5 s. The quick response may be attributed to the unique peroxidase-like catalytic activity of MOFs to H_2O_2 and the graphene nano-sheets facilitated direct electron transfer of mimetic enzyme to electrode. The resulting calibration plot is shown in the inset of Fig. 7, the linear regression equation is I (μA) = 0.492 + 0.0167C (μM) with the correlation coefficient (R) of 0.998.

View Article Online
DOI: 10.1039/C6TB00276E

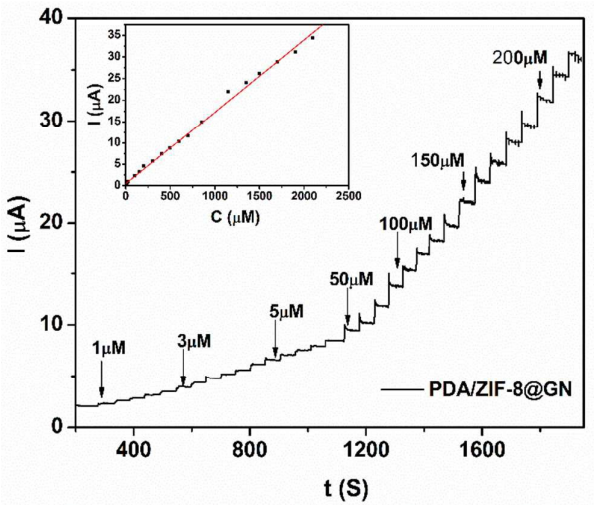

Fig. 7. Amperometric response of PDA/ZIF-8@rGO/GCE to successive addition of H_2O_2 in PBS (0.1 M, pH 7.0) at applied potential of 0.6 V.

3.4. Electrochemical detection of glucose at GOx/PDA/ZIF-8@rGO/GCE

Fig. 8A shows the CVs acquired at GOx/PDA/ZIF-8@rGO/GCE in 0.1 M PBS (pH 7.0) at scan rate ranged from 10 to 100 mV s^{-1}. A pair of redox peaks of GOx referred to the direct electron transfer between flavin adenine dinucleotide (FAD) and its reduced form, $FADH_2$, was observed at biosensor.[27] With the increase of the scan rate, both anodic and cathodic peak currents increase linearly as shown in the inset of Fig. 8A. In addition, with the increase of scan rate, the anodic peak potential slightly shifted to more positive potentials and cathodic peak potential slightly shifted to negative potentials. These electrochemical characteristics indicate that the reaction is a surface-controlled process. The linear regression equation is I_{pa} (μA) = 1.036 + 0.526ν (mV s^{-1}) with R_{pa} = 0.990 for anodic current, and I_{pc} (μA) = -4.661 - 0.507ν (mV s^{-1}), R_{pc} = 0.991 for cathodic current.

The effect of pH on the GOx/PDA/ZIF-8@rGO/GCE was studied by measuring the electrode response in 0.1 M PBS with pH values ranging from 3.0 to 7.0 and the

View Article Online
DOI: 10.1039/C6TB00276E

results were shown in Fig. 8B. With the increase of pH, the oxidation peak potential (E_{pa}) shifted negatively. The linear relationship between E_{pa} and pH was expressed by linear equation: E(V) = 0.374 - 0.0397 pH (R=0.996). The maximum oxidation peak current (I_{pa}) was obtained at pH 7.0 because the GOx denatured at low and high pH values. Hence, a phosphate buffer solution of pH 7.0 was chosen as the optimum pH value in electro-catalysis of glucose.[28]

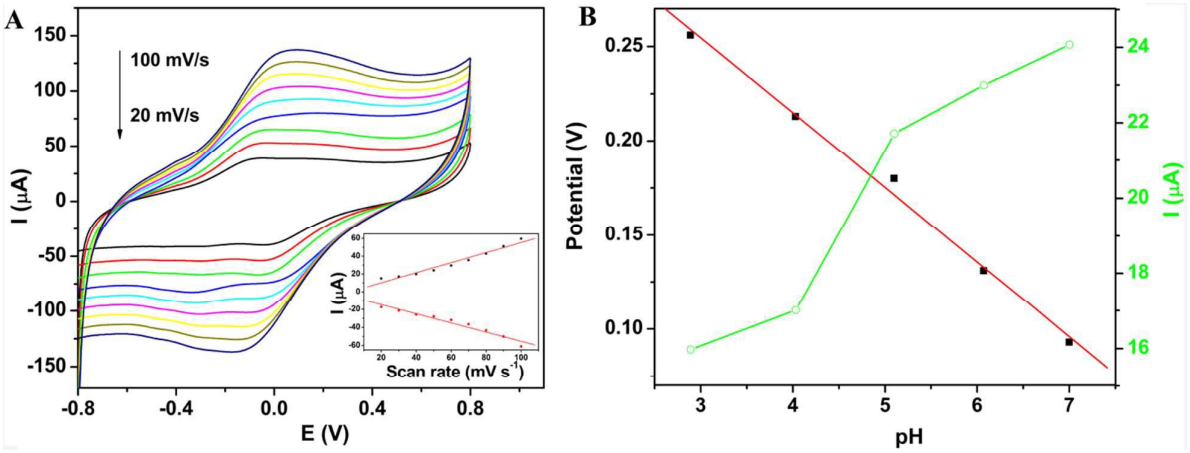

Fig. 8A. CVs of the PDA/ZIF-8@rGO/GCE in 0.1 mM PBS at scan rate of 10-100 mV s^{-1}. The inset shows the plots of anodic and cathodic peak currents *vs.* scan rates ; B. Effects of pH on E_{pa} and I_{pa} of the GOx/PDA/ZIF-8@rGO/GCE in 0.1 M PBS.

The glucose sensing performance of the GOx/PDA/ZIF-8@rGO/GCE was estimated by recording the amperometric response of the prepared sensor with successive addition of glucose to the stirring PBS (0.1 M pH 7.0) at 0.6 V, and the resulted typical i-t curve was shown in Fig. 9. An increase of the electro-catalytic current was observed for biosensor after each addition of an aliquot of glucose solution, with a time interval of 50 s. In addition, the current responses quickly and reached the steady-state current within 5 s for each injection of glucose. The noise

View Article Online
DOI: 10.1039/C6TB00276E

increased with the increase of glucose concentration might due to more and more intermediate species adsorbed onto the electrode. The current responses of the GOx/PDA/ZIF-8@rGO/GCE are linearly related the glucose concentration consist of two parts: one linear between 1.0 μM and 1.2 mM, linear regression equation: I (μA) = 2.532 + 0.161C (μM), R=0.997, and the detection limit of the biosensor was estimated to be 0.333 μM at a signal-to-noise ratio of 3. The other linear is in range from 1.2 mM to 3.6 mM, and the regression equation is I (μA) = 15.191 + 0.0096C (μM), R=0.994. The corresponding calibration curves are shown in inset of Fig. 9, and these results demonstrated that the GOx/PDA/ZIF-8@rGO/GCE had excellent electro-catalytic property for glucose and could be used as a promising electrochemical glucose biosensor. In order to estimate the analytical ability of the as-prepared biosensor, the detection performance for glucose was compared with those of previous electrochemical biosensors as presented in Table 1. The results indicated that the obtained biosensor in this work has comparable and even better performance than the others, demonstrating that PDA/ZIF-8@rGO/GCE has extraordinary application potential in determination of glucose.

View Article Online
DOI: 10.1039/C6TB00276E

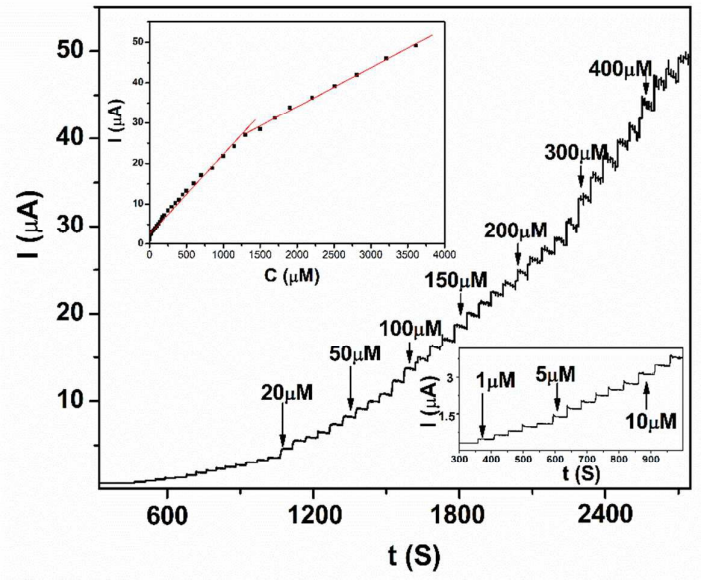

Fig. 9. Amperometric response of GOx/PDA/ZIF-8@rGO/GCE to successive addition of glucose in PBS (0.1 M, pH 7.0) at applied potential of 0.6 V.

Table 1 Comparison of analytical performance of glucose at different electrodes

Modified materials	Linear ranges (mM)	Detection limits (μM)	reference
GOx/graphene	0.1-10	10	29
GOx/graphene/PANI/Au	0.004-1.12	0.6	30
GOx/PtNP/PANI/Pt	0.01-8	0.7	31
GOx/PANI (microtubes)	0.004-0.8	0.8	32
Fe_3O_4/GOx/PPy	0.0005-34	0.3	3
GOx/MOFs/PtNPS	0.005-1.4	5	33
Au/cysteamine/GOD/chitosan	1.5-10.5, 10.5-27	50	28
ITO/ZnO/AuNPs/GOx	2.5-20	-	34
PDA/ZIF-8@rGO/GCE	0.001-1.2, 1.2-3.6	0.33	This work

3.5. Selectivity, stability and reproducibility of GOx/PDA/ZIF-8@rGO/GCE

As a key concern in biosensor applications, selective detection for the analyte among the interference from some coexisting electro-active species in real samples need to be studied. Here, the effect of some potential interferents such as ascorbic acid (AA), uric acid (UA), dopamine (DA) and fructose were tested one by one on the amperometric response of GOx/PDA/ZIF-8@rGO/GCE for 0.1 mM glucose. As

View Article Online
DOI: 10.1039/C6TB00276E

shown in Fig. 10, a significant enhancement of the curent and steady-state response potential reached after addition of glucose, on the contrary, none of above interferents caused any notable responses on the biosensor. Therefore, the GOx/PDA/ZIF-8@rGO/GCE biosensor exhibited a good selectivity for glucose over these molecules with similar structure or electro-activity. To demonstrate the reproducibility of the GOx/PDA/ZIF-8@rGO/GCE, the resulted sensor was successively scanned in 1 mM glucose PBS (0.1 M, pH 7.0) for 25 cycles, and no obvious changes were found in the peak current in the CV curves. Seven biosensors made in the same way were used to measure 1 mM glucose, the relative standard deviation (RSD) was 2.5% obtained by measurements. To test the long-term stability, the biosensor was stored in 0.1 M PBS (pH=7.0) at 4 ^{o}C in a refrigerator and investigated by measuring its response for 1 mM glucose over a 15 day period, the response current remained almost 95% of its initial current which illustrated that PDA/ZIF-8@rGO microcapsule provided a biocompatible microenvironment for the inside enzyme. Therefore, the results indicated that the GOx/PDA/ZIF-8@rGO/GCE biosensor showed excellent selectivity, reproducibility and stability for detection of glucose.

View Article Online
DOI: 10.1039/C6TB00276E

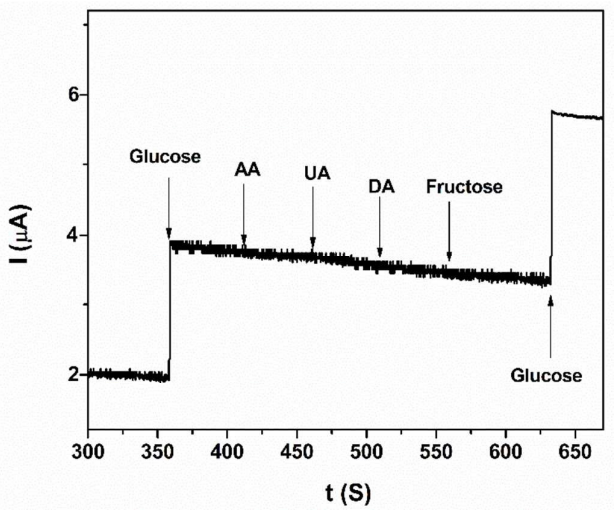

Fig. 10. Amperometric response of GOx/PDA/ZIF-8@rGO/GCE to addition of 0.1 mM glucose or 0.01 mM interferents in PBS (0.1 M, pH 7.0) at applied potential of 0.6 V.

3.6. Real sample determination

To illustrate the feasibility of the as-prepared biosensor in a biologically relevant matrix, glucose concentration in human serum samples have been measured by GOx/PDA/ZIF-8@rGO/GCE. Real samples determination was experimented by the standard addition method. The serum samples were diluted with PBS (0.1 M, pH 7.0) in order to fit into the linear ranges of glucose and avoid the interferences in the real samples, different amounts of known concentrations of glucose were spiked to each 5.0 mL of diluted serum samples, and measured under the optimal conditions. The experiment was studied by diluting the serum sample with PBS (0.1 M, pH 7.0) in order to fit into the linear ranges of glucose and avoid the interferences in the real samples, the different concentration of glucose were spiked to each 5.0 mL of diluted serum samples. All the obtained analytical results were summarized in Table 2. It was found that the recovery for assays of 0.01-2 mM glucose achieved 92.3%-110% with

View Article Online
DOI: 10.1039/C6TB00276E

the RSD values calculated to be less than 4%, implying that the GOx/PDA/ZIF-8@rGO/GCE biosensor is feasible for practical analysis.

Table 2 Determination of glucose in real samples using GOx/PDA/ZIF-8@rGO/GCE

Added (mM)	Serum samples Found (mM)	RSD (%)	Recovery (%)
0.01	0.011	2.05	110
0.05	0.051	1.45	102
0.1	0.097	3.13	97
0.5	0.491	3.04	98.2
1	0.923	3.91	92.3
1.5	1.49	1.46	99.3
2	2.02	1.02	101

4. Conclusion

A sensitive glucose biosensor based on the mimetic multi-enzyme system was fabricated by combing the mimetic enzyme (MOFs) and GOx. The PDA/ZIF-8 microcapsule, prepared with $CaCO_3$ templates, was not only used as the biocompatible and non-toxic support to immobilize GOx, but also worked as the mimetic enzyme due to the peroxidase-like property of ZIF-8. After the graphene nano-sheets were bonded to PDA/ZIF-8 microcapsule, the prepared sensor showed excellent electro-catalytic activity towards H_2O_2. Since GOx was immobilized in the microcapsule, a new amperometric glucose biosensor based on the mimetic multi-enzyme system has been developed. The resulted GOx/PDA/ZIF-8@rGO/GCE provided a promising strategy to construct high sensitive, stable and anti-interferential electrochemical biosensor for glucose detection. Plus with the biocompatibility of PDA and the high catalytic activity of ZIF-8, this effective electro-sensor based on the multi-enzyme system is promising to find widespread use in applications related to biomedicine, biosensor, and tissue engineering.

View Article Online
DOI: 10.1039/C6TB00276E

Acknowledgments

The authors gratefully acknowledge financial supports from the National Natural Science Foundation of China (No. 21304040), Natural Science Foundation of Gansu Province (1308RJYA027), Chinese Postdoctoral Funds (2013M532090), the National Natural Science Foundation of China (No. 21407071), and the Fundamental Research Funds for the Central Universities (lzujbky-2014-123).

View Article Online
DOI: 10.1039/C6TB00276E

References

1 M. Y. Wu, S. G. Meng, Q. Wang, W. Si, W. Huang and X. C. Dong, *ACS Appl. Mater. Interfaces,* 2015, **7**, 21089-21094.

2 K. Tian, M. Prestgard and A. Tiwari, *Mat. Sci. Eng. C-Mater.*, 2014, **41**, 100-118.

3 Z. P. Yang, C. J. Zhang, J. X. Zhang and W. B. Bai, *Biosens. Bioelectron.*, 2014, **51**, 268-273.

4 K. Hwa and B. Subramani, *Biosens. Bioelectron.*, 2014, **62**, 127-133.

5 Y. C. Tsai, S.C. Li and S. W. Liao, *Biosens. Bioelectron.,* 2006, **22**, 495-500.

6 X. L. Wang, Z. Y. Jiang, J. F. Shi, Y. P. Liang, C. H. Zhang and H. Wu, *ACS Appl. Mater. Interfaces,* 2012, **4**, 3476-3483.

7 C. Y. Tian, C. H. Zhang, H. Wu, Y. X. Song, J. F. Shi, X. L. Wang, X. K. Song, C. Yang and Z. G. Jiang, *J. Mater. Chem. B,* 2014, **2**, 4346-4355.

8 J. F. Shi, C. Yang, S. H. Zhang, X. L. Wang, Z. G. Jiang, W. Y. Zhang, X. K. Song and C. Y. Tian, *ACS Appl. Mater. Interfaces,* 2013, **5**, 9991-9997.

9 L. Zhang, J. F. Shi, Z. G. Jiang, Y. J. Jiang, S. Z. Qiao, J. Li, R. Wang, R. J. Meng, Y. Y. Zhu and Y. Zheng, *Green Chem.,* 2011, **13**, 300-306.

10 C. Hou, Y. Wang, H. Zhu and L. C. Zhou, *J. Mater. Chem. B,* 2015, **3**, 2883-2891.

11 X. L. Wu, J. Ge, C. Yan, M. Hou and Z. Liu, *Chem. Commun.*, 2015, **51**, 13408-13411.

12 X. Q. Wu, J. G. Ma, H. Li, D. M. Chen, W. Gu, G. M. Yang and P. Cheng, *Chem. Commun.*, 2015, **51**, 9161-9164.

13 F. Q. Luo, Y. L. Lin, L. Y. Zheng, X. M. Lin and Y. W. Chi, *ACS Appl. Mater. Interfaces*, 2015, **7**, 11322-11329.

14 S. Patra, T. H. Crespo, A. Permyakova, C. Sicard, C. Serre, A. Chaussé, N. Steunou and L.

View Article Online
DOI: 10.1039/C6TB00276E

Legrand, *J. Mater. Chem. B*, 2015, **3**, 8983-8992.

15 C. Hou, Y. Wang, Q. Ding, L. Jiang, M. Li, W. Zhu, D. Pan, H. Zhou and M. Z. Liu, *Nanoscale,* 2015, **7**, 18770-18779.

16 X. Wang, Q. X. Wang, Q. H. Wang, F. Gao, F. Gao, Y. Z. Yang and H. X. Guo, *ACS Appl. Mater. Interfaces*, 2014, **6**, 11573-11580.

17 Y. Wang, Y. Zhang, C. Hou and M. Z. Liu, *RSC Adv.,* 2015, **5**, 98260-98268.

18 Y. C. Pan, Y. Y. Liu, G. F. Zeng, L. Zhao and Z. P. Lai, *Chem. Commun.*, 2011, **47**, 2071-2073.

19 J. J. Zhou, P. Wang, C. X. Wang, Y. Goh, Z. Fang, P. Messersmith and H. W. Duan, *ACS Nano*, 2015, **9**, 6951-6960.

20 H. Zhou, W. Yao, G. Li, J. Wang and Y. Lu, *Carbon,* 2013, **59**, 495-502.

21 Y. X. Wang, S. H. Wang, H. Y. Niu, Y. R. Ma, T. Zeng, Y. Q. Cai and Z. F. Meng, *J. Chromatogr. A,* 2013, **1283**, 20-26.

22 J. N. Zheng, Z. Lin, G. Lin, H. H. Yang and L. Zhang, *J. Mater. Chem. B*, 2015, **3**, 2185-2191.

23 S. J. Kim and C. B. Park, *Langmuir,* 2010, **26**, 14730-14736.

24 F. K. Shieh, S. C. Wang, S. Y. Leo and K. C. W. Wu, *Chem. Eur. J.,* 2013, **19**, 11139-11142.

25 C. Cheng, S. Q. Nie, S. Li and H. Peng, *J. Mater. Chem. B,* 2013, **1**, 265-275.

26 S. X. Xu, H. L. Qi, S. Y. Zhou, X. F. Zhang and C. X. Zhang, *Microchim. Acta,* 2012, **4**, 535-541.

27 H. P. Peng, R. P. Liang, L. Zhang and J. D. Qiu, *Biosens. Bioelectron.*, 2013, **42**, 293-299.

28 Y. W. Zhang, Y. Q. Li, W. J. Wu, Y. R. Jiang and B. R. Hu, *Biosens. Bioelectron.,* 2014, **60**, 271-276.

29 P. Wu, Q. Shao, Y. Hu, J. Jin, Y. Yin, H. Zhang and C. Cai, *Electrochim. Acta,* 2010, **55**,

View Article Online
DOI: 10.1039/C6TB00276E

8606-8614.

30 Q. Xu, S. X. Gu, L. Jin, Y. E. Zhou, Z. Yang, W. Wang and X. Hu, *Sens. Actuators B*, 2014, **190**, 562-569.

31 D. Zhai, B. Liu, Y. Shi, L. Pan, Y. Wang, W. Li, R. Zhang and G. Yu, *ACS Nano*, 2013, **7**, 3540-3546.

32 L. Zhang, C. S. Zhou, J. J. Luo, Y. Y. Long, C. M. Wang, T. T. Yu and D. Xiao, *J. Mater. Chem. B*, 2015, **3**, 1116-1124.

33 S. Patra, T. Crespo, A. Permyakova, C. Sicard, C. Serre, A. Chausse, N. Steunou and L. Legrand, *J. Mater. Chem. B*, 2015, **3**, 8983-8992.

34 K. Tian, S. Alex, G. Siegel and A. Tiwari, *Mat. Sci. Eng. C-Mater.*, 2015, **46**, 548-552.